Photoacoustics 11 (2018) 36–45

Contents lists available at ScienceDirect

Photoacoustics

journal homepage: www.elsevier.com/locate/pacs

Research article

Photoacoustic imaging of integrin-overexpressing tumors using a novel ICG-based contrast agent in mice

Martina Capozza[a,c], Francesco Blasi[b], Giovanni Valbusa[b], Paolo Oliva[c], Claudia Cabella[c], Federica Buonsanti[c], Alessia Cordaro[c], Lorena Pizzuto[c], Alessandro Maiocchi[c], Luisa Poggi[c,*]

[a] Università degli Studi di Torino, Dipartimento di Biotecnologie Molecolari e Scienze per la Salute, Via Nizza 52, 10126, Torino, Italy
[b] Ephoran – Multi-Imaging Solutions, Via Ribes 5, 10010, Colleretto Giacosa, Torino, Italy
[c] Bracco Imaging SpA, Centro Ricerche Bracco, Via Ribes 5, 10010, Colleretto Giacosa, Torino, Italy

ARTICLE INFO

Keywords:
Indocyanine green
Tumor targeting
Contrast agents
Photoacoustic imaging
$\alpha_v\beta_3$-Integrin
Optoacoustic imaging

ABSTRACT

PhotoAcoustic Imaging (PAI) is a biomedical imaging modality currently under evaluation in preclinical and clinical settings. In this work, ICG is coupled to an integrin binding vector (ICG-RGD) to combine the good photoacoustic properties of ICG and the favourable $\alpha_v\beta_3$-binding capabilities of a small RGD cyclic peptidomimetic. ICG-RGD is characterized in terms of physicochemical properties, biodistribution and imaging performance. Tumor uptake was assessed in subcutaneous xenograft mouse models of human glioblastoma (U-87MG, high $\alpha_v\beta_3$ expression) and epidermoid carcinoma (A431, low $\alpha_v\beta_3$ expression). ICG and ICG-RGD showed high PA signal in tumors already after 15 min post-injection. At later time points the signal of ICG rapidly decreased, while ICG-RGD showed sustained uptake in U-87MG but not in A431 tumors, likely due to the integrin-mediated retention of the probe. In conclusion, ICG-RGD is a novel targeted contrast agents for PAI with superior biodistribution, tumor uptake properties and diagnostic value compared to ICG.

1. Introduction

Photoacoustic imaging (PAI) is a biomedical imaging modality based on laser-generated ultrasounds that has gained attention particularly over the last decade [1,2]. Of relevance, the most recent advancement in the PAI filed has been the development of Multispectral Optoacoustic Tomography (MSOT), in which the sample is irradiated (in a tomographic setup) with multiple wavelengths, allowing it to detect ultrasound waves emitted by different photoabsorbing molecules in the tissue, whether endogenous (oxygenated and deoxygenated hemoglobin, melanin) or exogenous (imaging probes, nanoparticles). Computational techniques such as spectral unmixing deconvolute the ultrasound waves emitted by these different absorbers, allowing each emitter to be visualized separately in the target tissue [3,4]. While the detection of endogenous chromophores has already been exploited in clinical settings (*i.e.*, Hemoglobin), the development and bench-to-bedside translation of exogenous agents is still lacking [5]. Fluorescent dyes developed for Optical Imaging (OI) applications can be exploited for PAI, particularly those with a high molar extinction coefficient and low fluorescence efficiency, as the non-radiative conversion of light energy to heat is maximized [6]. Indeed, the heptamethine cyanine dye Indocyanine green (ICG), clinically available for fluorescence angiography and liver function assessment by OI, is currently being evaluated off-label for photoacoustic imaging applications [7]. In recent clinical trials on melanoma patients [8,9], ICG was evaluated non-invasively using fluorescence imaging and multispectral optoacoustic tomography (MSOT) to detected non-invasively sentinel lymph nodes after intradermal injection in proximity of the primary tumor. While fluorescence imaging revealed only superficial nodes, PAI picked up ICG-positive lymph nodes up to a depth of 5 cm [8]. *In vivo* PAI of sentinel lymph node using ICG revealed comparable results with the gold standard ^{99m}Tc lymphoscintigraphy. The detection of metastatic melanoma lymphnode mapping using the photoacoustic signal of endogenous chromophore melanin granted 100% sensitivity compared to histopathology, but only 48% and 62% specificity *in vivo* and *ex vivo*, respectively [8]. This study showed that a non-invasive approach using photoacoustic imaging could reduce the number of patients with negative sentinel lymph nodes subjected to surgical excision. However, the specificity is still limited, probably due to the lack of a cancer-specific tracer able to discriminate between tumor and healthy tissues, as already reported in studies based on fluorescence imaging [10,11]. Integrins are adhesion proteins present at basal levels in normal tissues but are overexpressed in several types of cancer, particularly during tumor neoangiogenesis, [12,13]. Molecular imaging of integrins (*i.e.*,

* Corresponding author.
E-mail address: luisa.poggi@bracco.com (L. Poggi).

https://doi.org/10.1016/j.pacs.2018.07.007
Received 14 February 2018; Received in revised form 27 July 2018; Accepted 27 July 2018
Available online 03 August 2018

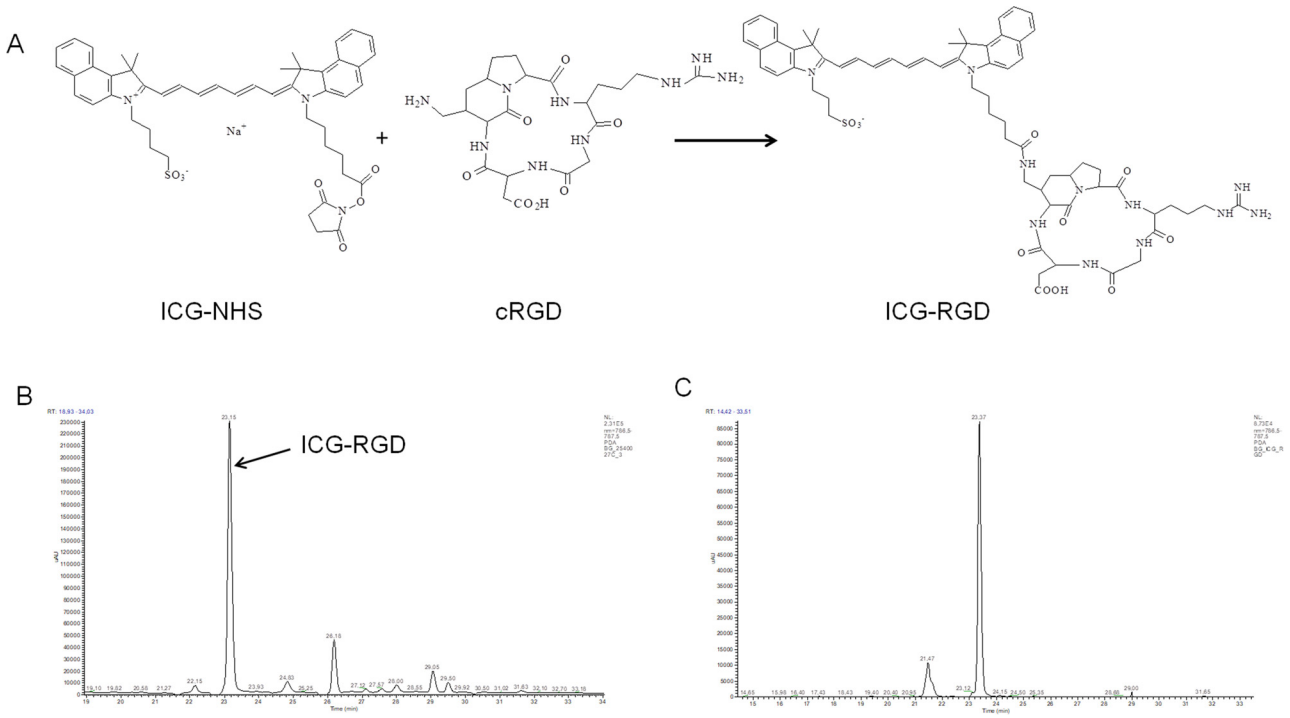

Fig. 1. Synthesis of ICG-RGD. A) Scheme of synthesis; B) UV–vis trace of HPLC chromatogram of ICG-am-cRGD in DMF before purification extracted at 787 nm; C) UV–vis trace of HPLC chromatogram of ICG-am-cRGD extracted at 787 nm in MilliQ/DMF 2:1 after purification.

$\alpha_v\beta_3$, $\alpha_v\beta_5$) has been extensively exploited for cancer detection, and several targeted contrast agents have been proposed for PET [14], MRI [15], ultrasound [16,17] and optical/photoacoustics imaging [18,19]. Small integrin-targeting near-infrared fluorescent probes carrying the detection moiety Arg-Gly-Asp (RGD) were proposed in the last years for *in vivo* cancer detection, but mainly for fluorescent imaging application [18–21]. Given the greater penetration depth capabilities of PAI compared to optical imaging, PAI may allow to image deeper tumor lesions, to detect non-invasively deep metastatic lymph node, and to facilitate the identification of residual disease underneath the tissue surface during surgery [22]. Therefore, targeted photoacoustic imaging could be a valid approach to increase specificity of detection particularly in those applications where near-infrared fluorescence imaging is sub-optimal. To this purpose, a novel integrin-targeting photoacoustic probe was synthesized to combine the good photoacoustic properties of ICG and the favourable $\alpha_v\beta_3$-binding capabilities of a cyclic RGD peptidomimetic moiety previously used for fluorescence imaging [23,24]. Here, the physicochemical properties (including albumin-binding properties), biodistribution and imaging performance of this novel contrast agent for photoacoustic imaging of cancer were evaluated and directly compared to ICG both *in vitro* and *in vivo*.

2. Material and methods

2.1. Synthesis and characterization of ICG-RGD

ICG-NHS ester (10 mg, 0.012 mmol, Intrace Medical) was first dissolved in dry N,*N*-Dimethylformamide, and then mixed with the peptidomimetic azabicycloalkane integrin-binding vector am-cRGD [23] (10 mg, 0.0186 mmol). After 24 h stirring in the dark, HPLC analytical control (YMC-Triart Phenyl column 250 × 4.6 mm 5 µm, 50–100% of acetonitrile in ammonium acetate buffer) was performed. The solution was then evaporated to obtain a green powder. A further purification was performed on reverse phase HPLC (Lichrosorb RP-8 250 × 25 mm 7 µm, 30 mL/min, with a gradient of ammonium acetate – acetonitrile, UV detection at λ = 780 nm). The solution was then evaporated and lyophilized three times. To characterize the product an HPLC-MS analysis was performed (YMC-Triart Phenyl 250 × 4.6 mm 5 µm, column temperature 40 °C, flow 1 mL/min, ammonium acetate and acetic acid and ACN). Data were processed using Xalibur software for qualitative and qualitative analysis. Purity was calculated from the area under the curve of the peaks detected at λ = 787 nm.

2.2. Cell line and animal models

Human glioblastoma cells (U-87MG), human epidermoid carcinoma (A431) and melanoma (WM-266) cells were supplied by ATCC. U-87MG and WM-266 cells were cultured in EMEM medium, A431 cells were cultured in DMEM high glucose medium; both media were supplemented with 10% FBS, 2 mM glutamine, 100 IU/mL penicillin and 100 µg/mL streptomycin. BALB/c nu/nu mice were provided by Charles River Italia Laboratories. Under isoflurane anaesthesia, mice were subcutaneously implanted in the right flank with either five million of A431 cells or two million of U-87MG cells. Imaging experiments were performed approximately 14 days after cells implantation. All the procedures involving the animals were conducted according to the national and international laws on experimental animals (L.D. 26/2014; Directive 2010/63/EU).

2.3. Imaging systems

The photoacoustic instrument used for this work was the VevoLAZR 2100 (Visualsonics), equipped with a transducer (Vevo LAZR LZ250) with a broadband ultrasound frequency of 13 MHz–24 MHz, producing an axial resolution of 75 µm. The optical imaging experiments were performed on IVIS Instrument SPECTRUM (Perkin Elmer), equipped with a CCD camera and a series of excitation (ex) and emission (em) filters. To image ICG and ICG-RGD, the optimal filter pair were 745 nm (ex) and 820 nm (em).

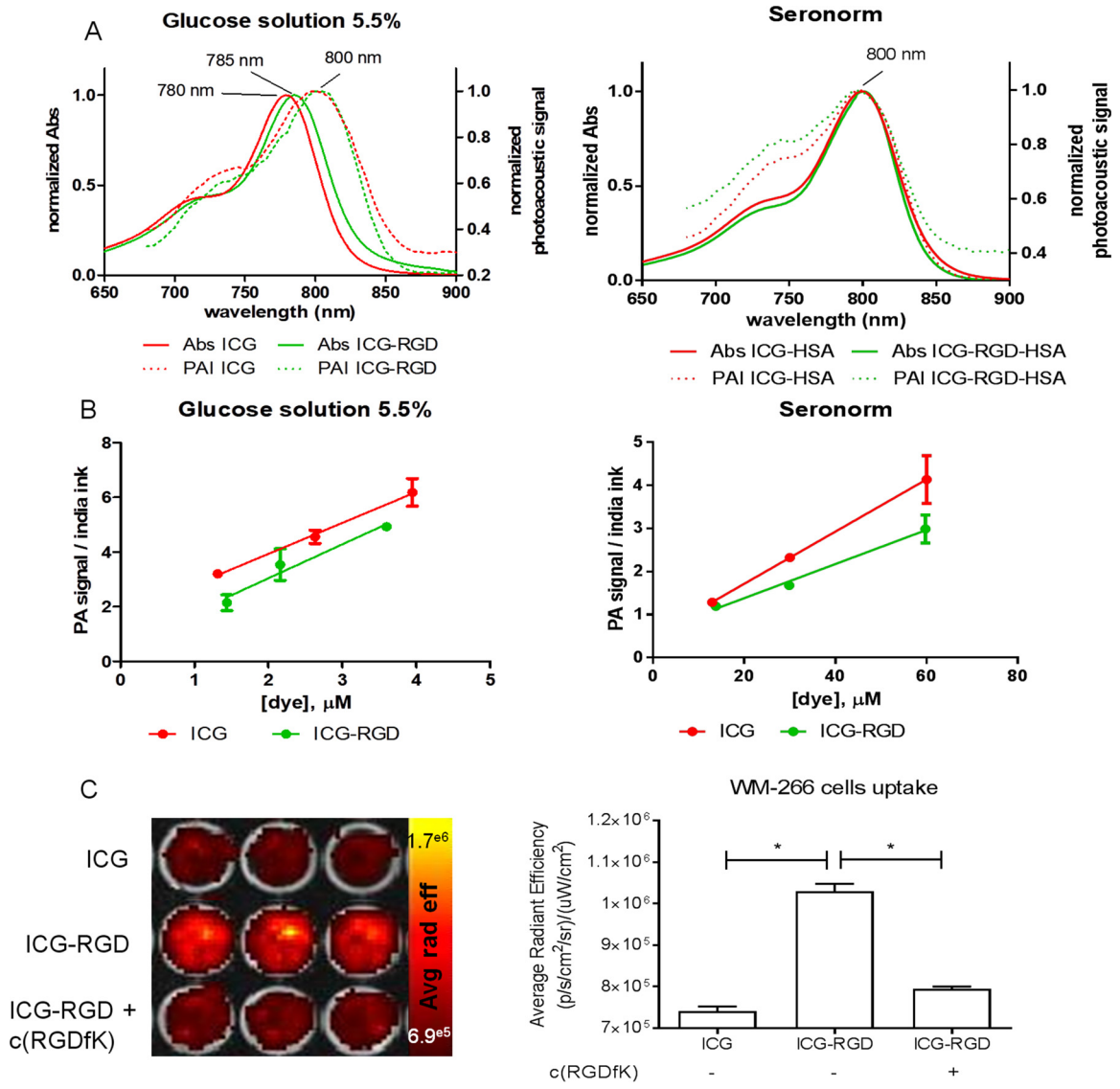

Fig. 2. Optical and photoacoustic characterization and WM-266 cells interaction. A) Absorbance (continuous line) and photoacoustic normalized spectra (dashed line) of ICG and ICG-RGD in glucose solution 5.5% (left) and albumin bound (right); B) Photoacoustic signal at maximum wavelength measured in glucose solution (left panel) and in human serum, after 1 h incubation at RT (right panel). C) Representative optical image (left) and quantification (right) of WM-266 cells interaction after incubation for 30 min with 1 μM of either ICG or ICG-RGD, with or without co-incubation with 100 μM of the unlabelled peptide c(RGDfK). *P < 0.0001, 1-way ANOVA followed by Bonferroni post-hoc test.

2.4. In vitro characterization

Dye solutions were freshly prepared by dilution in glucose solution 5.5% (for ICG-RGD, 5% DMSO was added to facilitate the solubilisation) and incubated (1 h, RT) in human serum (Seronorm™, HSA concentration: 47.8 g/L). A dual-beam Perkin Elmer Lambda 40 UV-VIS spectrophotometer was used to register the absorption spectra. The absolute fluorescence quantum yield measurements were carried out on the FluoroLog-3 1IHR-320 spectrofluorometer equipped with an F-3018 integrating sphere accessory (Horiba Jobin Yvon). The sample was excited with a 450 W Xenon Light Source at maximum absorption wavelength (780 nm). Detection was performed by cooled photomultiplier tubes (PMT-NIR). Dye solutions had an absorbance lower than 0.1 [25].

In order to evaluate the dye-HSA (lyophilized powder ≥97%, Sigma-Aldrich) binding constants, the UV-VIS spectra in the wavelength region 600–900 nm of dye solutions with increasing concentrations of HSA (0–225 μM) were recorded after incubation (1 h, RT). To extrapolate the association constant (K_A), the maximum absorbance of the dye-HSA complex at different HSA titrations was used to fit the equation reported below:

$$Abs = \frac{Ka\,[A]_{TOT} + Ka\,[B]_{TOT} + 1 - \sqrt{(Ka\,[A]_{TOT} + Ka\,[B]_{TOT} + 1)^2 - 4Ka^2\,[A]_{TOT}\,[B]_{TOT}}}{2Ka} \times (\varepsilon_{AB} - \varepsilon_B) + \varepsilon_B [B]_{TOT}$$

Where Abs is the measured absorbance, Ka is the association constant, A is HSA and B is the free dye, while ε_{AB} and ε_B are the molar extinction coefficient of the complex (dye-HSA) and molar extinction coefficient of the free dye.

For all the PA *in vitro* experiments, ultrasound frequency was set at 21 MHz, PA gain at 40 dB Photoacoustic spectra were acquired in the wavelength range from 680 nm to 970 nm with a step size of 5 nm, and persistence of 3. To register the photoacoustic spectra the solution was loaded in polyethylene tubes (PE-100) embedded in solidified agar (2% w/v, in milliQ water). An acoustic gel was used as coupling agent between the ultrasound transducer and the phantom. The photoacoustic signal of each dye was normalized by the signal of a diluted solution of

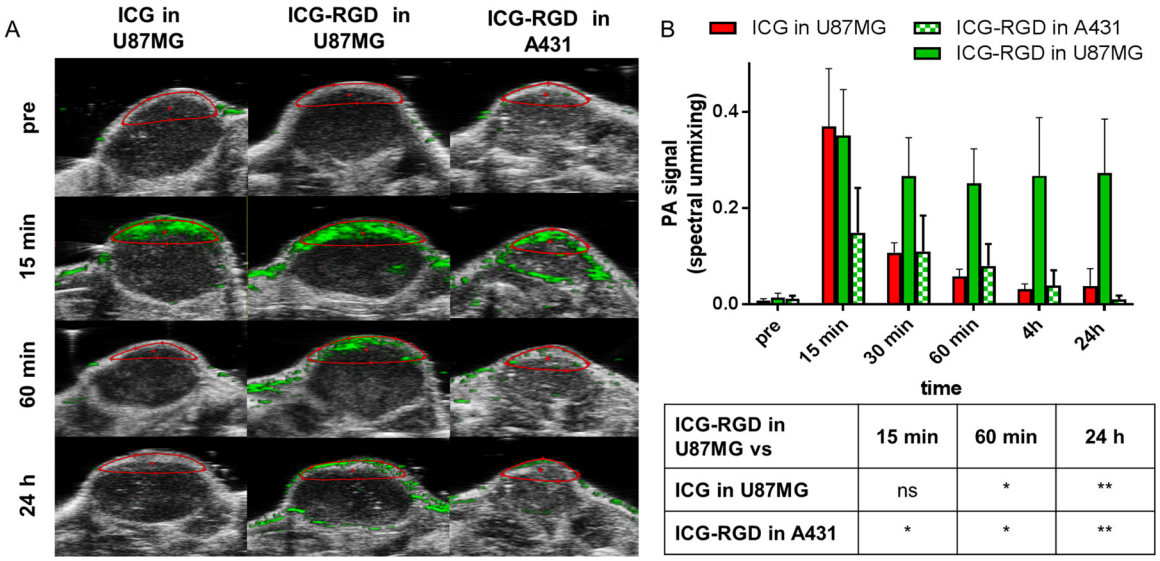

ICG-RGD in U87MG vs	15 min	60 min	24 h
ICG in U87MG	ns	*	**
ICG-RGD in A431	*	*	**

Fig. 3. *In vivo* photoacoustic imaging. A) Representative PA images of the tumor region acquired 15 min, 60 min and 24 h post injection and spectrally unmixed with VevoLAB. The ROIs used for data analysis are indicated in red; B) PA signal of tumor region at different timepoint after injection (n = 5/group). *P < 0.01, **P < 0.001, ns P > 0.05, 2-way ANOVA repeated measures followed by Bonferroni post-hoc test.

India Ink set as reference and reported as $\frac{PA_{CA}}{PA_{India\ Ink}}$. Photoacoustic signals at the maximum absorption wavelength of the contrast agents in glucose solution and serum were plotted *vs*. dye concentration to evaluate photoacoustic efficiency and the slopes were compared.

Integrin-mediated cell interaction of ICG-RGD was evaluated on the high $\alpha_V\beta_3$-expressing cell line WM-266 [26]. Non-conjugated ICG was used as negative control. 5×10^4 WM-266 cells were allowed to attach overnight to 96-well plates. ICG 1 μM (Cardiogreen, dye content 86%, Sigma-Aldrich) and ICG-RGD 1 μM were incubated at 37 °C for 30 min, with or without the addition of 100 μM of the high-affinity integrin-binding commercial peptide c(RGDfK) (Bachem). Then, the plate was washed three times with EBSS and analyzed with the IVIS Instrument SPECTRUM and the average radiance was quantified in each well.

2.5. ICG-RGD and ICG in U-87MG and A431 tumor bearing mice

ICG and ICG-RGD (200 nmol in 0.2 mL) were intravenously injected in the tail vein in U-87MG- and A431-bearing mice (n = 5/group). PAI acquisition parameters were: PA Gain 44 dB, persistence 3, spectrum from 680 to 970 nm, with step-acquisition every 5 nm. Photoacoustic spectra were acquired over a cross-section of the tumor at 10 min, 30 min and 1, 4 and 24 h after probes administration. *In vivo* OI experiments were performed 2 and 24 h after probe injection. After the last *in vivo* imaging acquisition and five minutes before sacrifice, mice were injected with FITC-albumin fluorescent dye solution (10 mg/mL, Sigma-Aldrich) at the dose of 100 mg/kg (administration volume 10 mL/kg) into the tail vein. For each group, tumor, brain, lung, liver, kidneys, heart and spleen were excised for *ex vivo* OI acquisitions. Tumors were embedded in OCT (Bio-Optica, Milano) medium and the entire tissue blocks were fresh-frozen in ice-cold isopentane. Cryosections obtained from the OCT blocks were visualized with the use of the Axio Zoom V16 (Carl Zeiss Microscopy GmbH) fluorescence microscope.

Photoacoustic image analysis was performed with the VevoLAB software package (Visualsonics). The signal intensity within the ROIs was reported as photoacoustic signal (spectral unmixing). For OI experiments, the analysis was performed with the Living Image IVIS software. The signal intensity was reported as average radiance efficiency $(p/s/cm^2/sr)/(\mu W/cm^2)$. ROIs were drawn in the tumor region. In order to be consistent with PAI measurements, where the tumor signal is not background-corrected, no background correction was used in the evaluation of OI experiments.

2.6. Ex-vivo tumor characterization

An additional cohort of animals (n = 4 for western blot and n = 4 for immunofluorescence) was used to further characterize the tumors. The same protocol adopted for tumor preparation for imaging (Section 2.2) was applied. Western blot was used to assess integrin expression in tumors by evaluating the biomarker subunit β_3 [27]. The total protein extract was loaded in a 10% polyacrylamide gel and electrophoresis in denaturing conditions (20% SDS) was carried out. Proteins within the gel were transferred onto a nitrocellulose membrane and subsequently blotted with the antibody anti-β_3 (Cell Signaling, Leiden, Germany). The specific signal generated by the anti-β_3 antibody was visualized as a single band at 87 kDa. The images of the labelled nitrocellulose were acquired with the ChemiDoc MP Imaging system and the area of the band relative to the β_3 expression level was quantified with the software Image Lab v.4.1. The resulted quantification of the β_3 subunit was normalized to the relative tumor weight. Immunofluorescence was performed to evaluate tumor vascularization by specific immunostaining of endothelium on tumor sections. Labeling was performed on fixed tissues slice incubating antibody anti-CD105 (Abcam, Cambridge, USA) 3 h at RT in 1% BSA. Afterwards, tissue slices were incubated with the secondary antibody.

2.7. Statistical analysis

Data are expressed as mean ± standard deviation. Differences between groups were analysed using unpaired, two-tailed Student's *t*-test, 1-way and 2-way analysis of variance (ANOVA) followed by Bonferroni post-hoc test, whenever appropriate. A p-value < 0.05 was considered significant.

3. Results

3.1. Synthesis and characterization of ICG-RGD

ICG was conjugated to cRGD exploiting the reaction between the NHS ester-activated dye and the primary amine of the molecular vector (Fig. 1A). The main peak corresponded to the expected reaction product, ICG-RGD (Fig. 1B, retention time: 23.15 min; *m/z*: 1250).

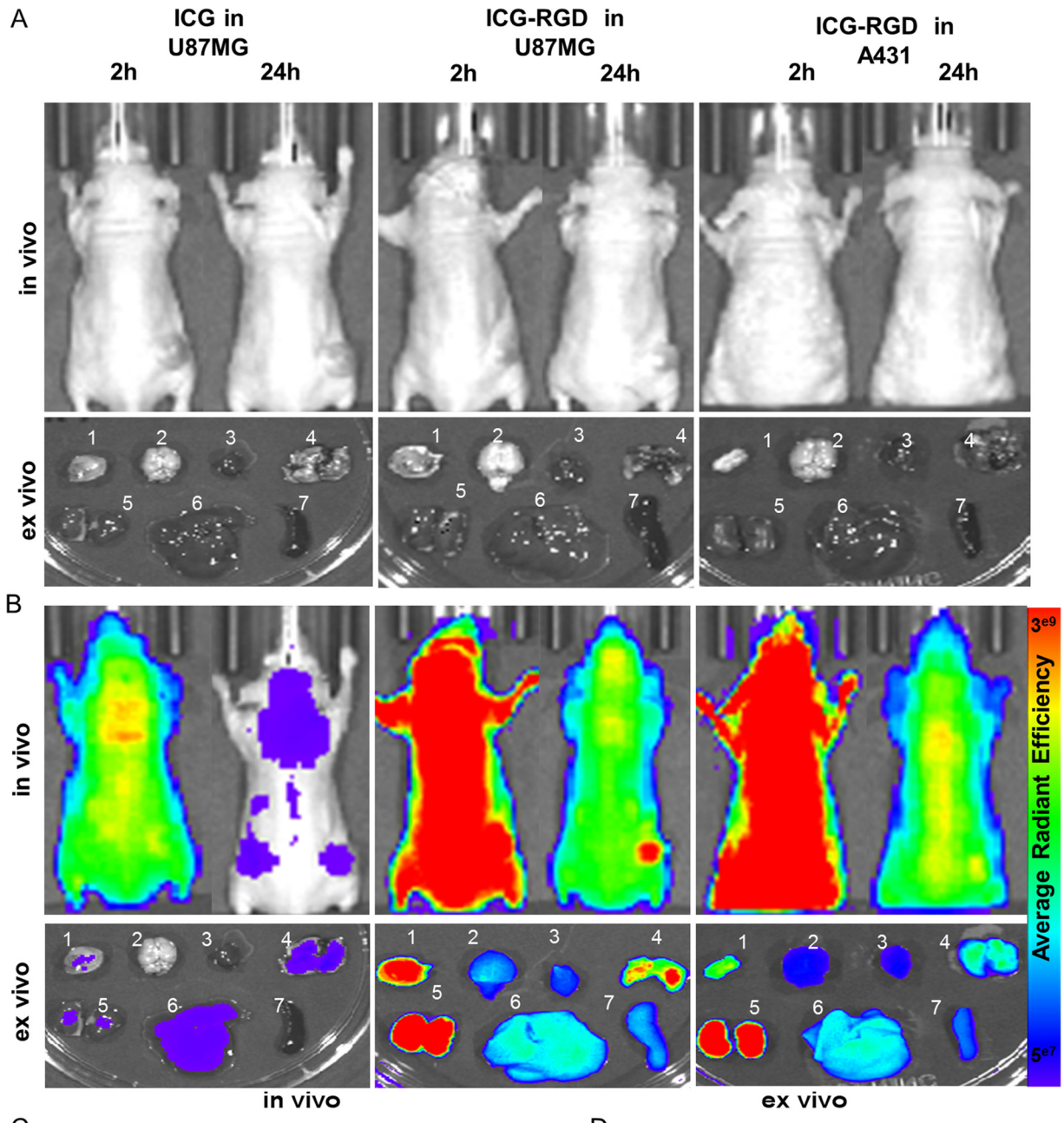

(caption on next page)

Fig. 4. *In vivo* and *ex vivo* optical imaging. A) Representative gray-scale *in vivo* optical imaging of tumor bearing mice 2 h (left panel) and 24 h (right panel) after administration of ICG and ICG-RGD (n = 5/group) in U-87MG and A431 tumor bearing mice. Lower panels represent *ex vivo* optical image of tumor (1), brain (2), heart (3), lung (4), kidney (5), liver (6) and spleen (7), and of A431- and U-87MG- tumor bearing mice injected with ICG and ICG-RGD; B) Representative *in vivo* optical images of tumor bearing mice 2 h (left panel) and 24 h (right panel) after administration of ICG and ICG-RGD (n = 5/group) in U-87MG and A431 tumor bearing mice. Lower panels represent *ex vivo* optical image of tumor (1), brain (2), heart (3), lung (4), kidney (5), liver (6) and spleen (7), and of A431- and U-87MG-tumor bearing mice injected with ICG and ICG-RGD. C) OI signal *in vivo* of tumor region at different timepoint after injection (n = 5/group). *P < 0.05, **P < 0.01, 2-way ANOVA repeated measures followed by Bonferroni post-hoc test. D) OI signal *ex vivo* of tumors after 24 h post injection (n = 5/group). § P < 0.001, 1-way ANOVA repeated measures followed by Bonferroni post-hoc test.

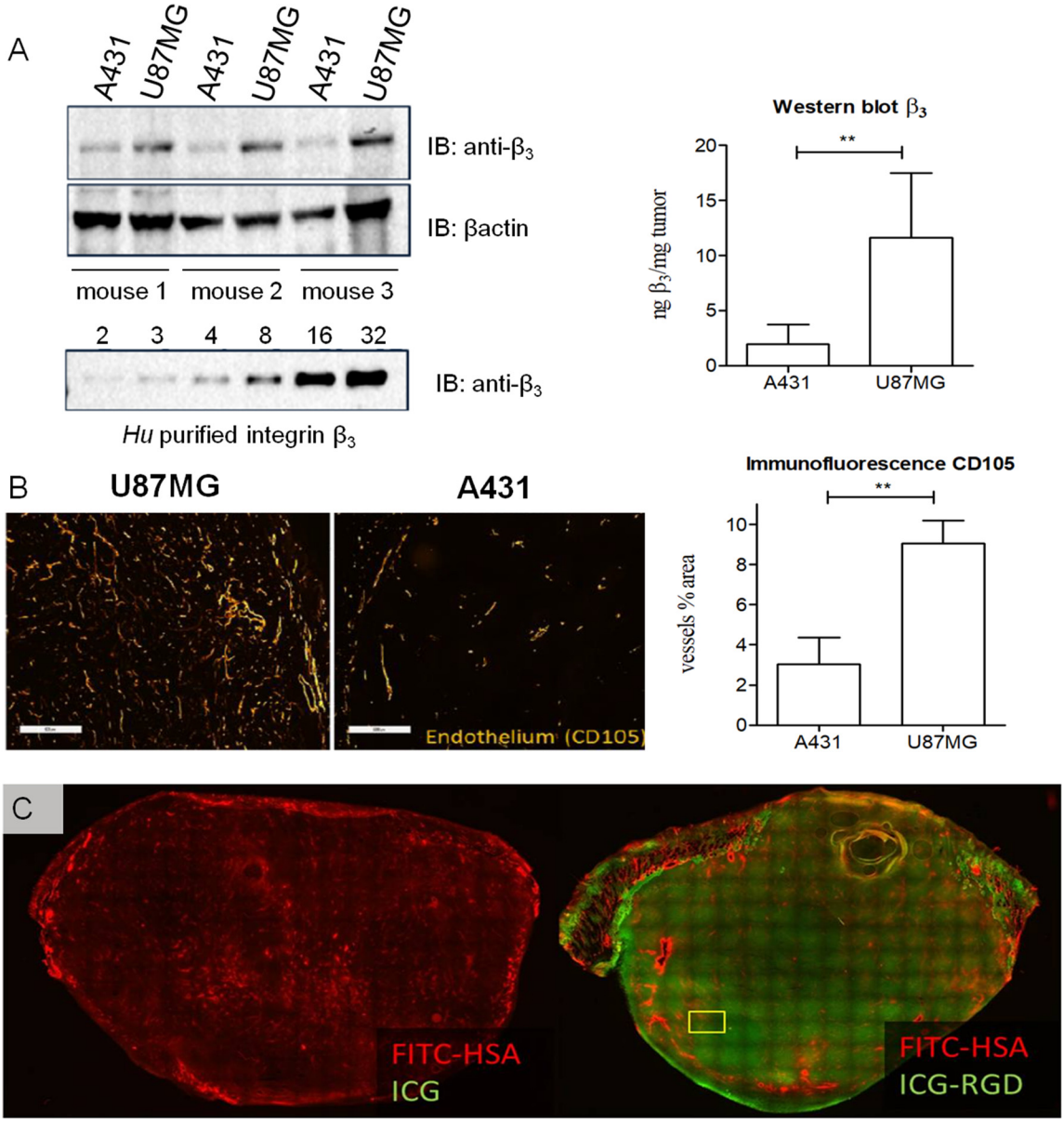

Fig. 5. Tumor characterization. A) Immunoblotting of U-87MG and A431 tumor extracts. A calibration curve of human purified integrin β_3 subunit was used to assess the protein content in the tumors, β-actin was used as loading control. The graph shows the amount of β_3 normalized to the tumor weight for U-87MG and A431 tumor (n = 4). B) Immunofluorescence staining of the endothelial marker CD105 on U-87MG and A431 tumor cryosections. The graph shows the percentage of area covered by CD105-positive vessels relative to the whole tumor area (n = 4). Scale bar: 500 μm. **P < 0.0001, unpaired, two-tailed Student's *t*-test. C) Fluorescence distribution of ICG and ICG-RGD in U-87MG tumor cryosections. A high fluorescence signal was detected in tumors from animals injected with ICG-RGD (right), while only low signal was visible after ICG administration (left).

Reaction by-products (ICG − COOH, RT 26.18 min, *m/z* 738; ICG-NHS, RT 29.05 min, *m/z* 828; ICG − $COOCH_3$, RT 29.50, min, *m/z* 745) were eliminated by HPLC purification with a final ICG-RGD purity of 83% (Fig. 1B and C). ICG and ICG-RGD showed comparable maximum absorption peak and comparable fluorescence quantum efficiency both in glucose solution (1.5 ± 0.04% and 1.22 ± 0.11%) and serum (7.76 ± 0.59% and 7.10 ± 0.28%). The fluorescence efficiency of ICG and ICG-RGD showed a 5-fold increase when incubated in Seronorm^{TM} compared to glucose solution. Moreover, ICG and ICG-RGD showed similar affinity to HSA ($K_A = 5.04 \times 10^5 \pm 5.6 \times 10^4\ M^{-1}$ for ICG and $2.19 \times 10^5 M^{-1}$ for ICG-RGD). Both contrast agents showed a maximum photoacoustic peak at 800 nm in glucose solution 5.5% and serum

(Fig. 2A). Both ICG-RGD and ICG showed a strong PA signal in glucose solution, but their PA signal in serum decreased substantially, probably due to the serum protein interactions and consequent fluorescence quantum yield increase. The photoacoustic signal *vs.* concentration slope (expressed as μM^{-1}) in glucose solution was 1.13 ± 0.06 for ICG and 1.24 ± 0.24 for ICG-RGD; while in human serum it was 0.060 ± 0.002 for ICG and 0.040 ± 0.004 for ICG-RGD (Fig. 2B). The interaction of ICG-RGD to integrin receptors was confirmed by incubation of ICG-RGD and ICG on high $\alpha_v\beta_3$-expressing WM-266 cells. The WM-266 cells displayed a greater fluorescent signal after incubation with ICG-RGD than ICG, suggesting an integrin-dependent interaction. Moreover, incubation of cells with both ICG-RGD and the integrin-binding peptide c(RGDfK) reduced the cell interaction of ICG-RGD, almost to the level observed after incubation with unlabeled-ICG (Fig. 2C).

3.2. Tumor uptake in animal models of human cancer

In U-87MG tumor bearing mice the photoacoustic signal after injection of ICG and ICG-RGD peaked 15 min post-injection, but already at 60 min ICG showed a 70% signal reduction compared to 15 min, while the signal of ICG-RGD was still elevated (Fig. 3). ICG-RGD showed sustained tumor uptake up to 24 h post-injection, likely due to the integrin-mediated accumulation of the probe (Fig. 3B). ICG-RGD was then tested in A431-tumor bearing mice. In these tumors, a strong signal was observed at 15 min post-injection with a statistically significant difference compared to baseline, while at later timepoints the signal rapidly decreased. At 24 h post injection, the ICG-RGD signal in U-87MG was 25 times greater than the signal in A431 (Fig. 3B). OI experiments were performed to corroborate the photoacoustic imaging results (Fig. 4). ICG showed a strong signal after 2 h but at 24 h post injection the signal decreased substantially. ICG-RGD showed similar behaviour in both A431 and U-87MG tumors after 2 h, but a greater signal was observed in U-87MG after 24 h. *Ex vivo* imaging of harvested organs showed that 24 h post-injection ICG accumulated mainly in liver and kidney. ICG-RGD showed a strong signal in the kidneys, while a higher signal was observed in U-87MG tumors compared to A431, supporting *in vivo* results (Fig. 4).

U-87MG tumors displayed higher levels of integrin β3 expression compared with A431 tumors, as evaluated by western blot experiments (Fig. 5A). Immunofluorescence images highlighted high and widespread vascularization in U-87MG tumors, while on A431 sections such vascularization was limited. The percentage of area covered by blood vessels in tumor section was about 8% for U-87MG, while a smaller stained area was detected for A431 tumors (< 4%) (Fig. 5B). Cryosections obtained from U-87MG tumors excised 24 h after ICG and ICG-RGD injection were further evaluated to assess the microscopic distribution of the probes (Fig. 5C), together with the distribution of FITC-HSA, which was used as an estimation of the permeability of the tumor. For ICG, only a patchy and weak signal was observed at 24 h post-injection, while a strong ICG-RGD signal was present throughout the cryosection confirming the imaging findings. Of note, while CD105 reports for vascularization, FITC-HSA assess the permeability of the vessels in the tumor, hence accounting for the distribution of the probes, due to their specific HSA-binding capability.

4. Discussion

PAI has gained increasing interest in recent years in the field of diagnostic applications. The primary contrast mechanism explored in photoacoustic imaging has been and still is that of endogenous molecules and tissue components such as hemoglobin, oxy-hemoglobin, melanin, bilirubin, lipids, and water. Very few exogenous contrast agents have been evaluated for PAI up to clinical level. Of those, even less possess targeted properties for molecular imaging applications. Several small molecule dyes that absorb in the NIR window can be used for PAI to report on normal physiology as well as pathophysiological events. For example, Indocyanine green (ICG) [7], Evans blue and Methylene blue [28] are clinically available dyes and may be adopted for PAI. However, these molecules show several drawbacks that make them not ideal for PAI. ICG has very short blood half-life (< 3-5 min in human), low photostability, and low solubility in aqueous media with strong tendency to form aggregates that strongly limits its use. Evans blue and Methylene blue have been used for PAI but are limited by their relatively blue-shifted absorption peak [5]. Other NIR dyes, not approved for human use, like IRDye800CW [29], AlexaFluor750 [30], ATTO740 [31], IR780 [32] and others [33,34] have been recently investigated as photoacoustic probes, either as is or chemically bound to biomolecules to generate targeted contrast agents. All these examples show the feasibility of using small NIR dyes for PAI and for tumor detection. In this work, the novel photoacoustic contrast agent ICG-RGD was synthesized, characterized *in vitro* and evaluated in animal models of human cancer. The novel probe shows superior biodistribution, tumor uptake properties and diagnostic value compared to the untargeted dye ICG. Furthermore, the novel probe allows to discriminate noninvasively between tumors with high and low integrin $\alpha_v\beta_3$ expression, therefore it may be useful as contrast agent for photoacoustic molecular imaging of tumor angiogenesis.

The first step in the evaluation process of novel contrast agents for photoacoustic imaging is the assessment of the optical properties. Favourable properties for a photoacoustic contrast agent are high molar extinction coefficient and low fluorescent quantum yield [5]. However, besides the abovementioned physicochemical properties, other determinants, such as kinetics of non-radiative deactivation, triplet state contribution and photobleaching, need to be considered when determining a molecule's ability to convert light energy into heat [35], as required to generate high PA signal. Optical properties are strongly affected by the interaction of the dye with the biological matrix. For example, the increase of fluorescence quantum yield after albumin binding is an effect well characterized and reported in literature [36]. This phenomenon is due to the placement of the fluorophore into a rigid environment (bound to albumin) and to the different polarity of the media [37]. Indeed, the fluorescence quantum yield of ICG and ICG-RGD strongly increases after incubation in albumin. Thus, ICG and ICG-RGD showed a photoacoustic signals in serum significantly lower than in glucose solution due to their strong interaction with plasma proteins [36] and consequent increase of fluorescent quantum yield. Besides the optical properties, albumin binding affinity strongly affects the biodistribution and tumor uptake of the dyes. In living biological systems albumin is the predominant protein in blood, and have been known to act as a carrier to transport a variety of biologically-active species, including drugs [38]. However, despite the similar albumin binding affinities, ICG-RGD and ICG displayed different body clearance and tumor uptake, suggesting that chemical modifications (*i.e.*, coupling with a RGD-moiety) may strongly affect biodistribution and blood circulation time of ICG-based fluorophores, probably because a reduced capitation from the liver. Of note, the optical and photoacoustic properties of ICG are not significantly affected by the coupling with the RGD cyclic peptide. The photoacoustic signal of ICG-RGD in glucose solution and serum is indeed comparable to free ICG. Both ICG-RGD and ICG showed high PA signal in U-87MG tumors already after 15 min, suggesting that in this early vascular phase the two contrast agents diffuse similarly. One can postulate that this similarity is due to the comparable albumin-binding properties of the two molecules that strongly affect the early enhancement phase of contrast agents. Differently, at later time-points, only the ICG-RGD signal remained elevated in the integrin-overexpressing tumors, suggesting greater tumor retention possibly due to target-mediated cell internalization.

ICG-RGD strongly accumulated in U-87MG tumors thanks to the high vascularization of this xenograft model, which facilitates the distribution of the probe in the tumor tissue, and to the overexpression of the target $\alpha_v\beta_3$ integrin, which contributes to the specific retention of

the fluorescent contrast agent. The *in vitro* interaction assay confirmed the specific binding of ICG-RGD to integrin-overexpressing cells, particularly the strong reduction of cell uptake after co-incubation with the well-known competitor cyclic pentapeptide c(RGDfK). Not surprisingly, ICG-RGD showed different behaviour after injection in A431 (low $\alpha_v\beta_3$ expression [39]) and U-87MG (high $\alpha_v\beta_3$ expression [40]) tumor-bearing mice. The PA signal of ICG-RGD in A431 tumors rapidly decreased after injection, while the PA signal in U-87MG plateau already after 30–60 min and is stable up to 24 h post injection. At this time-point, the ICG-RGD signal in U-87MG was 25 times greater than the signal in A431. Optical imaging experiments confirmed these results; after 24 h, a greater signal was registered for U-87MG compared to A431. The first attempt to image $\alpha_v\beta_3$ with RGD-based photoacoustic probes was conducted by de la Zerda et al. in 2008 [41]. They showed that single-walled carbon nanotubes (SWNT) conjugated with cyclic Arg-Gly-Asp (RGD) peptides can be used as a contrast agent for photoacoustic imaging of integrin-overexpressing tumors. However, the clinical translation of a nanosystems like SWNT may be challenging. Recently, Zhang et al. reported the development and evaluation of an Atto740-labeled cysteine knot peptide, which selectively binds integrin $\alpha_v\beta_6$ with high affinity, for photoacoustic and fluorescence imaging. The new dual-modality probe may find clinical application in cancer diagnosis and intraoperative imaging of integrin $\alpha_v\beta_6$-positive tumors [42]. In 2017 Grimm et al proposed a black hole quencher® (BHQ) bound to an integrin binding vector, and demonstrate its efficacy in U-87MG tumors bearing mice performing imaging with a high-resolution raster-scan optoacoustic mesoscopy (RSOM) [43].

It has to be pointed out that integrin photoacoustic imaging has been already demonstrated with MSOT [16a]. In this seminal work, a commercially available Near-infrared (NIR) fluorescent preclinical agent, (Perkin Elmer) was used for MSOT imaging of tumor angiogenesis. The Integrisense750 probe has been specifically developed for optical imaging applications, and it is therefore characterized by a high quantum yield, making it suboptimal for PAI applications. The superior imaging capabilities of the MSOT setup allowed indeed for the visualization of the probe in the preclinical lesions. The ICG-RGD probe presented in this work relies on the physico-chemical characteristics of the ICG dye, which are known to be more suitable for PA imaging. Thanks to our RGD peptidomimetic moiety that has been specifically developed and synthetized in house, we have been able to design an optimized probe for PAI applications, and we have been able to visualize it *in vivo* in a hand-held (*i.e.* non-tomographic) setup.

The application field of these integrin targeted probes is enormous. The ICG-RGD could find application in diagnostic imaging and fluorescence guided surgery.

4.1. Limitations of the study

Shortcomings of this work include the lack of direct evidence for active targeting and uptake of ICG-RGD in *in vitro* experiments with cells overexpressing $\alpha_v\beta_3$ integrins. We were not able to perform uptake experiments on ICG-RGD due to the very low sensitivity of our instrumentation at the ICG absorption and emission wavelengths. However, blocking experiments performed with the integrin-binding peptide c(RGDfK) reduced the cell interaction of ICG-RGD as assessed by *in vitro* OI experiments, almost to the level observed after incubation with unlabelled-ICG. These findings suggest an integrin-dependant interaction of ICG-RGD with WM-266 cells.

Another important limitation is related to the limited number of animals and the high mass dose of probe used for *in vivo* imaging experiments. The high mass dose was needed to detect photoacoustic signal *in vivo* because the limited sensitivity of the detection system. Nonetheless, a superior imaging performance was observed for the targeted probe ICG-RGD compared to the dye ICG for detecting tumor angiogenesis in integrin-overexpressing xenografts. Furthermore, *in vivo* photoacoustic imaging showed strong signal only at the edge of the tumor, suggesting poor probe penetration. However, a strong accumulation of the probe was clearly visible throughout the tumor in *ex vivo* sections. This discrepancy can be related to a suboptimal reconstruction of the photoacoustic signal in a deeper region of the tumor, with higher tissue attenuation and probably a lower probe concentration compared to the outmost regions of the tumor. This uneven distribution of the probe in the tumor is confirmed by the visualization of FITC-HSA, which was used as an estimation of the permeability of the tumor

We have tried to overcome such limitations by restricting our PAI analysis on ROIs close to the PAI/US probe, by validating our results with *ex vivo* techniques and, most importantly, by performing supportive OI experiments both *in vivo* and *ex vivo*. All our experimental findings (including PAI results) allowed us to confirm that ICG-RGD is selectively retained in tumors overexpressing $\alpha_v\beta_3$ integrins.

5. Conclusions

A novel integrin-targeting molecular probe for photoacoustic imaging based on well-known and clinically available dye ICG was successfully synthetized and evaluated *in vitro* and in animal models of human cancer. Such proof-of-concept may pave the road to the development of new targeted contrast agents with optical, physicochemical and biological properties optimized for photoacoustic imaging.

Conflict of interest

Martina Capozza is a former employee of Bracco Imaging SpA. Federica Buonsanti, Claudia Cabella, Alessia Cordaro, Alessandro Maiocchi, Paolo Oliva, Lorena Pizzuto and Luisa Poggi are employees of Bracco Imaging SpA.

Funding

This research did not receive any specific grant from funding agencies in the public, commercial, or not-for-profit sectors.

Acknowledgements

We thank Simona Ghiani for fruitful discussions, Mariangela Boccalon for the quantum yield measurements and Chiara Martano for providing the HPLC methods for ICG-RGD purification and characterization.

References

[1] S. Zackrisson, S.M. van de Ven, S.S. Gambhir, Light in and sound out: emerging translational strategies for photoacoustic imaging, Cancer Res. 74 (4) (2014) 979–1004.
[2] L.V. Wang, S. Hu, Photoacoustic tomography: in vivo imaging from organelles to organs, Science 335 (6075) (2012) 1458–1462.
[3] V. Ntziachristos, D. Razansky, Molecular imaging by means of multispectral optoacoustic tomography (MSOT), Chem. Rev. 110 (5) (2010) 2783–2794.
[4] A. Taruttis, V. Ntziachristos, Advances in real-time multispectral optoacoustic imaging and its applications, Nat. Photon. 9 (2015) 219.
[5] J. Weber, P.C. Beard, S.E. Bohndiek, Contrast agents for molecular photoacoustic imaging, Nat. Methods 13 (8) (2016) 639–650.
[6] G.P. Luke, D. Yeager, S.Y. Emelianov, Biomedical applications of photoacoustic imaging with exogenous contrast agents, Ann. Biomed. Eng. 40 (2) (2012) 422–437.
[7] A. Miyata, T. Ishizawa, M. Kamiya, A. Shimizu, J. Kaneko, H. Ijichi, J. Shibahara, M. Fukayama, Y. Midorikawa, Y. Urano, N. Kokudo, Photoacoustic tomography of human hepatic malignancies using intraoperative indocyanine green fluorescence imaging, PLoS One 9 (11) (2014) e112667.
[8] I. Stoffels, J. Dissemond, T. Pöppel, D. Schadendorf, J. Klode, Intraoperative fluorescence imaging for sentinel lymph node detection: prospective clinical trial to compare the usefulness of Indocyanine Green vs technetium Tc 99m for identification of sentinel lymph nodes, JAMA Surg. 150 (7) (2015) 617–623.
[9] I. Stoffels, S. Morscher, I. Helfrich, U. Hillen, J. Lehy, N.C. Burton, T.C. Sardella, J. Claussen, T.D. Poeppel, H.S. Bachmann, A. Roesch, K. Griewank, D. Schadendorf, M. Gunzer, J. Klode, Metastatic status of sentinel lymph nodes in melanoma determined noninvasively with multispectral optoacoustic imaging, Sci. Transl. Med.

7 (317) (2015) 317ra199.
[10] D. Holt, O. Okusanya, R. Judy, O. Venegas, J. Jiang, E. DeJesus, E. Eruslanov, J. Quatromoni, P. Bhojnagarwala, C. Deshpande, S. Albelda, S. Nie, S. Singhal, Intraoperative near-infrared imaging can distinguish cancer from normal tissue but not inflammation, PLoS One 9 (7) (2014) e103342.
[11] S. Keereweer, J.D. Kerrebijn, P.B. van Driel, B. Xie, E.L. Kaijzel, T.J. Snoeks, I. Que, M. Hutteman, J.R. van der Vorst, J.S. Mieog, A.L. Vahrmeijer, C.J. van de Velde, R.J. Baatenburg de Jong, C.W. Löwik, Optical image-guided surgery–where do we stand? Mol. Imaging Biol. 13 (2) (2011) 199–207.
[12] J.S. Desgrosellier, D.A. Cheresh, Integrins in cancer: biological implications and therapeutic opportunities, Nat. Rev. Cancer 10 (1) (2010) 9–22.
[13] J.F. Marshall, I.R. Hart, The role of alpha v-integrins in tumour progression and metastasis, Semin. Cancer Biol. 7 (3) (1996) 129–138.
[14] A.J. Beer, R. Haubner, M. Sarbia, M. Goebel, S. Luderschmidt, A.L. Grosu, O. Schnell, M. Niemeyer, H. Kessler, H.J. Wester, W.A. Weber, M. Schwaiger, Positron emission tomography using [18F]Galacto-RGD identifies the level of integrin alpha(v)beta3 expression in man, Clin. Cancer Res. 12 (13) (2006) 3942–3949.
[15] D.A. Sipkins, D.A. Cheresh, M.R. Kazemi, L.M. Nevin, M.D. Bednarski, K.C. Li, Detection of tumor angiogenesis in vivo by alphaVbeta3-targeted magnetic resonance imaging, Nat. Med. 4 (5) (1998) 623–626.
[16] H. Leong-Poi, J. Christiansen, A.L. Klibanov, S. Kaul, J.R. Lindner, Noninvasive assessment of angiogenesis by ultrasound and microbubbles targeted to alpha(v)-integrins, Circulation 107 (3) (2003) 455–460.
[17] Q. Hu, X.Y. Wang, L.K. Kang, H.M. Wei, C.M. Xu, T. Wang, Z.H. Wen, RGD-targeted ultrasound contrast agent for longitudinal assessment of Hep-2 tumor angiogenesis in vivo, PLoS One 11 (2) (2016) e0149075.
[18] J. Cao, S. Wan, J. Tian, S. Li, D. Deng, Z. Qian, Y. Gu, Fast clearing RGD-based near-infrared fluorescent probes for in vivo tumor diagnosis, Contrast Media Mol. Imaging 7 (4) (2012) 390–402.
[19] E. Herzog, A. Taruttis, N. Beziere, A.A. Lutich, D. Razansky, V. Ntziachristos, Optical imaging of cancer heterogeneity with multispectral optoacoustic tomography, Radiology 263 (2) (2012) 461–468.
[20] M.L. Li, J.T. Oh, X.Y. Xie, G. Ku, W. Wang, C. Li, G. Lungu, G. Stoica, L.V. Wang, Simultaneous molecular and hypoxia imaging of brain tumors in vivo using spectroscopic photoacoustic tomography, Proc. IEEE 96 (3) (2008) 481–489.
[21] Z. Cheng, Y. Wu, Z. Xiong, S.S. Gambhir, X. Chen, Near-infrared fluorescent RGD peptides for optical imaging of integrin alphavbeta3 expression in living mice, Bioconjug. Chem. 16 (6) (2005) 1433–1441.
[22] T.T.W. Wong, R. Zhang, P. Hai, C. Zhang, M.A. Pleitez, R.L. Aft, D.V. Novack, L.V. Wang, Fast label-free multilayered histology-like imaging of human breast cancer by photoacoustic microscopy, Sci. Adv. 3 (5) (2017) e1602168.
[23] S. Lanzardo, L. Conti, C. Brioschi, M.P. Bartolomeo, D. Arosio, L. Belvisi, L. Manzoni, A. Maiocchi, F. Maisano, G. Forni, A new optical imaging probe targeting αVβ3 integrin in glioblastoma xenografts, Contrast Media Mol. Imaging 6 (6) (2011) 449–458.
[24] L. Manzoni, L. Belvisi, D. Arosio, M. Civera, M. Pilkington-Miksa, D. Potenza, A. Caprini, E.M. Araldi, E. Monferini, M. Mancino, F. Podestà, C. Scolastico, Cyclic RGD-containing functionalized azabicycloalkane peptides as potent integrin antagonists for tumor targeting, ChemMedChem 4 (4) (2009) 615–632.
[25] C. Würth, M. Grabolle, J. Pauli, M. Spieles, U. Resch-Genger, Relative and absolute determination of fluorescence quantum yields of transparent samples, Nat. Protoc. 8 (8) (2013) 1535–1550.
[26] M. Pisano, I. DE Paola, V. Nieddu, I. Sassu, S. Cossu, G. Galleri, A. Del Gatto, M. Budroni, A. Cossu, M. Saviano, G. Palmieri, L. Zaccaro, C. Rozzo, In vitro activity of the αvβ3 integrin antagonist RGDechi-hCit on malignant melanoma cells, Anticancer Res. 33 (3) (2013) 871–879.
[27] M. Barczyk, S. Carracedo, D. Gullberg, Integrins, Cell Tissue Res. 339 (1) (2010) 269–280.
[28] A. Garcia-Uribe, T.N. Erpelding, A. Krumholz, H. Ke, K. Maslov, C. Appleton, J.A. Margenthaler, L.V. Wang, Dual-modality photoacoustic and ultrasound imaging system for noninvasive sentinel lymph node detection in patients with breast cancer, Sci Rep. 5 (2015) 15748.
[29] A.B. Attia, C.J. Ho, P. Chandrasekharan, G. Balasundaram, H.C. Tay, N.C. Burton, K.H. Chuang, V. Ntziachristos, M. Olivo, Multispectral optoacoustic and MRI co-registration for molecular imaging of orthotopic model of human glioblastoma, J. Biophotonics 9 (7) (2016) 701–708.
[30] S. Bhattacharyya, S. Wang, D. Reinecke, W. Kiser, R.A. Kruger, T.R. DeGrado, Synthesis and evaluation of near-infrared (NIR) dye-herceptin conjugates as photoacoustic computed tomography (PCT) probes for HER2 expression in breast cancer, Bioconjug. Chem. 19 (6) (2008) 1186–1193.
[31] J. Levi, A. Sathirachinda, S.S. Gambhir, A high-affinity, high-stability photoacoustic agent for imaging gastrin-releasing peptide receptor in prostate cancer, Clin. Cancer Res. 20 (14) (2014) 3721–3729.
[32] Q. Yang, H. Cui, S. Cai, X. Yang, M.L. Forrest, In vivo photoacoustic imaging of chemotherapy-induced apoptosis in squamous cell carcinoma using a near-infrared caspase-9 probe, J. Biomed. Opt. 16 (11) (2011) 116026.
[33] Y. Chen, S. Dhara, S.R. Banerjee, Y. Byun, M. Pullambhatla, R.C. Mease, M.G. Pomper, A low molecular weight PSMA-based fluorescent imaging agent for cancer, Biochem. Biophys. Res. Commun. 390 (3) (2009) 624–629.
[34] S. Bhattacharyya, N. Patel, L. Wei, L.A. Riffle, J.D. Kalen, G.C. Hill, P.M. Jacobs, K.R. Zinn, E. Rosenthal, Synthesis and biological evaluation of panitumumab-IRDye800 conjugate as a fluorescence imaging probe for EGFR-expressing cancers, Medchemcomm 5 (9) (2014) 1337–1346.
[35] J. Levi, S.R. Kothapalli, T.J. Ma, K. Hartman, B.T. Khuri-Yakub, S.S. Gambhir, Design, synthesis, and imaging of an activatable photoacoustic probe, J. Am. Chem. Soc. 132 (32) (2010) 11264–11269.
[36] M.Y. Berezin, S. Achilefu, Fluorescence lifetime measurements and biological imaging, Chem. Rev. 110 (5) (2010) 2641–2684.
[37] J. Pauli, T. Vag, R. Haag, M. Spieles, M. Wenzel, W.A. Kaiser, U. Resch-Genger, I. Hilger, An in vitro characterization study of new near infrared dyes for molecular imaging, Eur. J. Med. Chem. 44 (9) (2009) 3496–3503.
[38] K. Awasthi, G. Nishimura, Modification of near-infrared cyanine dyes by serum albumin protein, Photochem. Photobiol. Sci. 10 (4) (2011) 461–463.
[39] C. Zhang, M. Jugold, E.C. Woenne, T. Lammers, B. Morgenstern, M.M. Mueller, H. Zentgraf, M. Bock, M. Eisenhut, W. Semmler, F. Kiessling, Specific targeting of tumor angiogenesis by RGD-conjugated ultrasmall superparamagnetic iron oxide particles using a clinical 1.5-T magnetic resonance scanner, Cancer Res. 67 (4) (2007) 1555–1562.
[40] F. Kiessling, J. Huppert, C. Zhang, J. Jayapaul, S. Zwick, E.C. Woenne, M.M. Mueller, H. Zentgraf, M. Eisenhut, Y. Addadi, M. Neeman, W. Semmler, RGD-labeled USPIO inhibits adhesion and endocytotic activity of alpha v beta3-integrin-expressing glioma cells and only accumulates in the vascular tumor compartment, Radiology 253 (2) (2009) 462–469.
[41] A. De la Zerda, C. Zavaleta, S. Keren, S. Vaithilingam, S. Bodapati, Z. Liu, J. Levi, B.R. Smith, T.J. Ma, O. Oralkan, Z. Cheng, X. Chen, H. Dai, B.T. Khuri-Yakub, S.S. Gambhir, Carbon nanotubes as photoacoustic molecular imaging agents in living mice, Nat. Nanotechnol. 3 (9) (2008) 557–562.
[42] C. Zhang, R. Kimura, L. Abou-Elkacem, J. Levi, L. Xu, S.S. Gambhir, A cystine knot peptide targeting integrin αvβ6 for photoacoustic and fluorescence imaging of tumors in living subjects, J. Nucl. Med. 57 (Oct. (10)) (2016) 1629–1634.
[43] K. Haedicke, C. Brand, M. Omar, V. Ntziachristos, T. Reiner, J. Grimm, Sonophore labeled RGD: a targeted contrast agent for optoacoustic imaging, Photoacoustics 6 (2017) 1–8.

Martina Capozza, Ph.D obtained her Master degree in Molecular Biotechnology and Molecular Imaging at the Molecular Biotechnology Center at the University of Turin in October 2013. She earned a Ph.D. in Pharmaceutical and Biomolecular sciences at Bracco Imaging Research Center in collaboration with the University of Turin in March 2017. During this time, she focused on evaluation of the physico-chemical properties, biodistribution and imaging performance of different contrast agents for photoacoustic and optical imaging, particularly near infrared (NIR) absorbing dyes and dye-loaded nanosystems. From 2017, she started to work as a postdoc in Preclinical Imaging Laboratory under the supervision of Prof Aime.

Francesco Blasi, Ph.D. PharmD in 2007, received his PhD in Pharmacology and Biochemistry in 2012 from University of Calabria. He was Research Fellow for 5 years at Massachusetts General Hospital and Harvard Medical School, working on therapeutic and diagnostic agents in the fields of neuroscience and cardiovascular medicine, before moving to University of Turin in 2015. Consultant for Ephoran Multi Imaging Solutions s.r.l. from 2016, his current research focuses on the preclinical development of novel contrast agents for translation in clinical oncology.

Giovanni Valbusa, Dr. obtained his Master degree in Environmental Sciences in May 2003 at the University of Milan, Italy. He has been working for Bracco Imaging s.p.a from 2003 to 2013 as scientific researcher in the BioImaging lab and as biostatistician for the Test Facility department. Consultant for Ephoran Multi Imaging Solutions s.r.l. from 2013, his current research focuses on biomedical images analysis for radiomics applications and methods development for fluorescence and photoacoustic imaging.

Paolo Oliva, Dr. obtained his Master degree in Industrial Biotechnology in April 2008 at the University of Milan, Italy. He has had a postgraduate education in Pharmacological Research at IRCCS "Mario Negri" Institute for Pharmacological Research and several work experiences in pharmaceutical and biotech companies like Isagro Biofarming, Cell Therapeutics and Transgenic Operative Products. He has been working in Bracco Imaging since 2013 as scientific researcher in the BioImaging Department. He was involved in an European-funded project (NanoAthero) focalizing his activity in preclinical studies on atherosclerotic lesions. His work is currently focused on the development of new molecular imaging probes for different applications, in particular for imaging of oncological diseases, exploiting his expertise in Magnetic Resonance, Optical and Photoacustic Imaging.

Claudia Cabella, Ph.D. obtained her Master degree in Chemistry at the Department of Animal Biology in March 1996 at the University of Turin, Italy. She earned a Ph.D. in Biochemistry at the Department of Medicine and Experimental Oncology at the same University in February 2000. She has been working in Bracco Imaging SpA since 2003, currently managing the Preclinical Imaging Laboratory in the Italian research center of the company. Her primary area of expertise is Molecular Imaging, mainly focused on Magnetic Resonance and Optical Imaging and preparation of animal models. Her work is currently focused on the development of new molecular imaging probes for different applications and modalities, in particular for the imaging of oncological diseases and inflammation.

Federica Buonsanti, Ph.D. obtained her Master degree in Chemistry and Pharmaceutical Technology at the Pharmaceutic and Chemistry Department in July 2001 at the University of Messina, Italy. She received a Ph.D. in Pharmaceutical Sciences at the University of Turin, Italy, in February 2004. She has been working in Bracco Research Center Chemistry department since 2007 in both research and process development area, currently managing the Chemistry group in the same center. Her work is mainly direct to research and development of chemical entities as probe for diagnostic imaging solutions.

Alessia Cordaro, Dr. graduated in Biotechnology with a Bachelor Degree and in Industrial Biotechnology with a Master Degree at University of Turin (Italy), working on a thesis concerning the development of a recombinant protein for the treatment of Systemic Lupus Erythematous. She is a Ph.D. candidate in pharmaceutical and biomolecular science at University of Turin, with a project regarding the development of probes for imaging guided oncological surgery. She has been working in Bracco Imaging SpA since 2012 and her main activities are focused on the biological characterization of new optical imaging probes for cancer and atherosclerosis imaging.

Lorena Pizzuto, Dr. obtained her Master degree in Chemistry at the Organic Chemistry Department in December 2007 at the University of Turin, Italy. She took up her career in March 2008 as Junior Researcher in small companies, as responsible of synthesis of peptide-libraries (used as antimicrobials) and small molecules (used as topical treatments for inflammatory skin diseases). She has been working in Bracco Imaging SpA since 2014 as Senior Researcher in the Chemistry Department in the Italian research center of the company. Her work is currently focused on the synthesis, purification and characterization of new molecules for different applications and modalities, in particular for diagnostic imaging of oncological diseases and inflammation.

Alessandro Maiocchi, Dr. graduated in Industrial Chemistry in 1989 at the Science Faculty of the University of Milan. He has worked in the Bracco Group companies since 1990 covering different roles in R&D. Currently he is the Deputy of the Global R&D at Bracco Imaging. From 2004–2010 he had served as contract professor at the Dept. of Biotechnology and Molecular Sciences at the University of Varese in Italy. His current research activity is focused on the design and development of small and nanosized probes for molecular imaging applications in combination with therapies using Magnetic Resonance, Ultrasound, Photoacustic and Nuclear Imaging. He is member of several societies and author of more than 100 scientific publications on international journals and conference proceedings in the field of drug design, contrast agents characterization, pharmaceutical product development and imaging methods.

Luisa Poggi, Ph.D. obtained her Master degree in Chemistry at the Organic Chemistry Department in October 1999 at the University of Florence, Italy. She earned a Ph.D. in Chemistry at the same University in January 2003. She has been working in Bracco Imaging SpA since 2008, currently managing the BioImaging Department in the Italian research center of the company. Her primary area of expertise is Molecular Imaging, mainly focused on Magnetic Resonance, Optical and Photoacustic Imaging. Her work is currently focused on the development of new molecular imaging probes for different applications and modalities, in particular for the imaging of oncological diseases and inflammation.